Design of SIS Mixers for SMA 400 - 520 GHz Band

C. T. Li[1], C. M. Chang[1], M. J. Wang[1], and S. C. Shi[2]
[1]Institute of Astronomy and Astrophysics, Academic Sinica
Taipei 10617, Taiwan
[2]Purple Mountain Observatory
Nanjing, China 210008

***Abstract* - SIS junction mixers were designed for SMA 400 – 520 GHz band, which is similar to ALMA band 8 (380 – 500 GHz). Two schemes were used to tune out the parasitic capacitance of the junction. When shunt inductors were employed, the input resistance is equal to R (close to R_n), much higher than $R/(\omega RC)^2$ when series inductors were used. This facilitates the impedance matching between the junction and the waveguide probe. Waveguide probe design was varied to achieve a low feed-point impedance to match the junction resistance. The optimal feed-point impedances for lower receiver noise temperature were also discussed.**

I. Introduction

The Submillimeter Array (SMA)[1,2], constructed by Smithsonian Astrophysical Observatory (SAO) and Institute of Astronomy and Astrophysics, Academia Sinica (ASIAA) is a radio interferometer of eight 6-m antennas. Receivers incorporating superconductor-insulator-superconductor (SIS) mixers are being used for observations through major submillimeter atmospheric windows from 180 GHz to 900 GHz. This paper describes the design of SIS mixers for one target frequency band (400-520 GHz). The emphasis of this work is to compare mixer designs with two different tuning schemes and explore the optimum matching for lower receiver noise temperature over the entire band. Considering low LO power available at high frequencies, single-junction designs were adopted.

II. Waveguide-Microstrip Probe Design

We adopted the mixer block designed by E. Tong *et. al.* A detailed drawing of the center portion of the mixer block is given in Fig. 1. The dimensions are about 65% of those of the 250 - 350 GHz band block. The reduced height waveguide section (0.55 x 0.138 mm) has a fixed backshort, measuring 0.17 mm in depth. The fused quartz mixer chip, measuring 0.250 x 0.050 x 2.276 mm, will be clamped between the horn section and the mixer block back piece in a suspended microstrip configuration. The thickness of the substrate is reduced from 0.060 mm to 0.050 mm during simulation to avoid higher order (non-TEM) modes of propagation along the microstrip transmission lines.

We used a bow-tie probe[3] with its feed point located at the center of the waveguide, as shown in Fig. 2. The RF chokes following the low-impedance sections of the probe present an open at RF to the probe. By shortening the lengths of the low impedance sections of the probe, the feed-point impedance could be decreased. However, to accommodate the circuit consisting of the SIS junction, tuning circuits, and impedance transformers, one side of the probe is extended. The shape of the probe also has some effect on the feed-point impedance. In general, broader probes (larger θ in Fig. 5) yield lower impedances. This configuration, together with the RF chokes, produces a driving point impedance of about 26 Ω – j 23 Ω at 460 GHz, shown as the blue trace in Fig. 3.

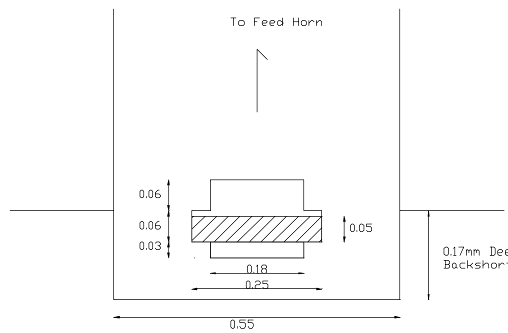

Figure 1. Sectional view of the mixer block center portion. The quartz substrate is hatched. The cross section of the suspended microstrip and the fixed backshort of the block are shown. All dimensions are in mm.

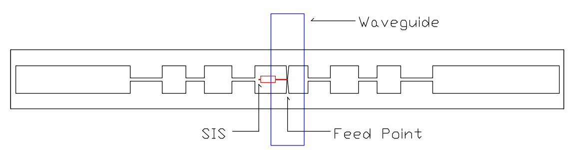

Figure 2. Top view of the mixer chip sitting in a channel along the E-plane of the waveguide.

The waveguide-microstrip probe was simulated using a 3D EM field simulator (Ansoft HFSS). During simulation, the depth of the backshort was reduced to rotate the locus of the feed-point impedance onto the real axis of the Smith chart, shown as the red trace in Fig. 3. However, after reducing the backshort depth, the impedance locus becomes so extended on the Smith chart, and to be compatible with SAO during array operation, we choose to adopt the same mixer block design. The reactance of the feed point impedance can be matched by adjusting the electrical lengths of the impedance transformers between the SIS junction and the feed point as illustrated in the following sections.

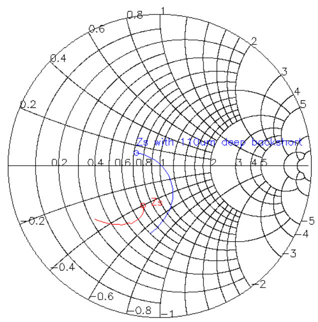

Figure 3. The locus of the junction feed point impedance (in blue), and that with a reduced back short (in red) from 400 GHz to 520 GHz. Circles mark the impedances at 400 GHz.

III. INDUCTIVELY TUNED SIS JUNCTIONS

Fig. 4 shows the equivalent circuits of two different schemes to tune out the junction parasitic capacitance, along with their corresponding optimum source resistance. Series transmission line inductors were widely used because of compactness of the tuning structure. This topology also lends itself to distributed junction design. However, after the capacitance is tuned out, the remaining resistance is equal to $R' = R/(\omega RC)^2$, much lower than R when $(\omega RC)^2 >> 1$. It usually requires two sections of quarter wavelength impedance transformers to bring the input impedance up to the level of few tens of ohms to match the feed-point impedance, as shown in Fig. 5. On the other hand, with a shunt inductor, the input impedance of the tuned junction is equal to R, which is on the order of junction normal state resistance R_n. Thereby, only one section of impedance transformer is needed. With fewer sections of impedance transformer, the noise induced by the transmission line loss can be reduced.

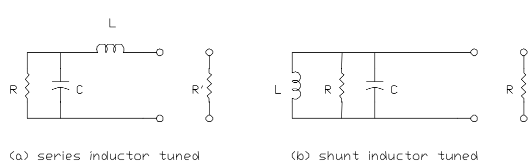

Figure 4. Equivalent circuits of (a) a series-inductor tuned junction, and (b) a shunt-inductor tuned junction, where C represents the junction capacitance, R is the junction resistance, and $R' = R / (\omega RC)^2$.

The series-inductor-tuned configuration corresponds to Fig. 1 (b) in [4] with $\omega RC \sim 4$ and $\omega L/R \sim 0.3$ for the junction we used in the simulation. The shunt-inductor-tuned case can be referred to Fig. 1 (c) in [4] with L = 0. Despite the difference in input impedances looked into the tuned junctions, both structures have similar bandwidths when terminated with their corresponding optimum source resistance. To increase the bandwidth, it would be necessary to reduce the value of ωRC or adopt multi-junction configurations.

Figure 6 shows how the input impedance Z_{inLO} evolves after each section of transmission lines. The input impedance Z_{inLO} is calculated by taking into account the complex current response of the SIS junction at each LO frequency, associated with G_{LO}^0 in [5]. The value could be quite different from junction's input impedance at signal frequencies Z_{in}, which is derived from the inversion of junction's admittance matrix. The Z_{in} at signal frequencies is related to G_s^0 in [5].

In Fig. 6, it is clear that after the series inductor, the imaginary part of junction admittance is mostly cancelled, while the remaining resistance is on the order of 1 Ω. After two sections of quarter wavelength impedance transformers, the input impedance Z_{inLO3} is close to the complex conjugate of the feed-point impedance Z_s. The lengths of transformers were adjusted so that the resulting input impedance locus is enclosing Z_s*. The simulation is done using the 5-port approximation to the quantum mixer theory[6] and an analytical model for thin-film superconducting microstrip lines[7]. The design comprises Nb/Al-AlO_x/Nb tunnel junctions integrated with Nb/SiO_2/Nb microstrip tuning circuits. The junction is characterized by a normal state resistance R_n of 19.5 Ω, J_c of 10 kA/cm^2, and the junction size of 1.25 μm in diameter, corresponding to a junction capacitance of 90 fF

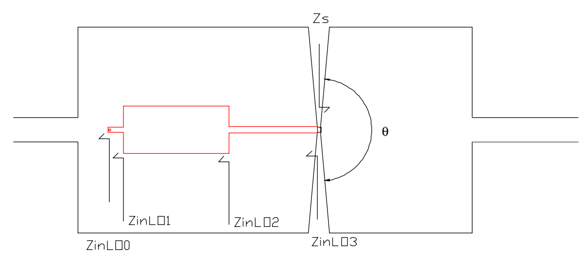

Figure 5. Tuning structure and impedance transformers for a series-inductor tuned SIS junction, where $Z_{inLO\,i}$, i = 1, 2, and 3, is the input impedance looked toward the junction after each section of transmission line, and Z_s is the feed point impedance.

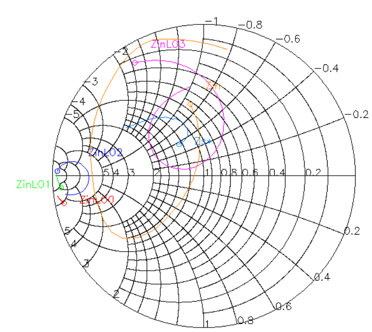

Figure 6. Input impedance loci looked into the junction, Z_{inLO0} and after each section of transmission line ($Z_{inLO\,i}$, i = 1, 2, and 3). Z_{in} is the input impedance at signal frequencies. Z_s* is the complex conjugate of the feed point impedance. Circles indicate the impedances starting from 380 GHz (to 540 GHz).

For the shunt-inductor-tuned configuration in Fig. 7, a quarter-wavelength low impedance open stub presents an RF short to the shunt inductor (made of a short, high-impedance transmission line). After the inductor tunes out the junction capacitance, the remaining resistance is about 18 Ω, while the optimum resistance derived from an empirical formula[5] ,

$$G_s = 1/2 + 1/(4\omega),$$

is about 22 Ω. Then one section of transformer is placed between the junction and the feed point. The length of the transformer is less than a quarter wavelength so that the final input impedance is located around Z_s*. The impedance loci are shown in Fig. 8 along with Z_s*.

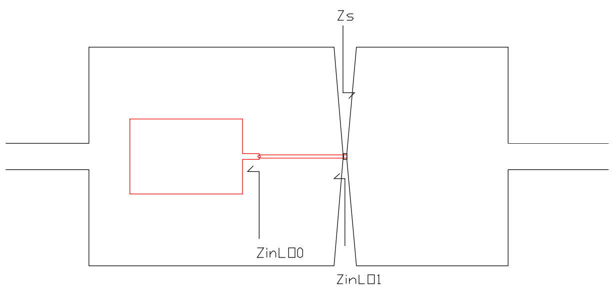

Figure 7. Tuning structure and impedance transformers for a shunt-inductor tuned SIS junction.

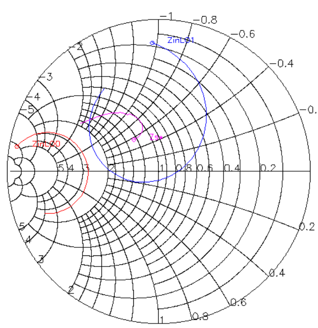

Figure 8. Input impedance Z_{inLO} loci looked into the tuned junction and after the impedance transformer, along with the complex conjugate of the feed point impedance Z_s* from 380 GHz to 540 GHz.

IV. OPTIMUM FEED POINT IMPEDANCE FOR LOW RECEIVER NOISE TEMPERATURE

To explore the optimum feed point impedance for lower receiver noise temperature, it is clear to look at the SIS junction tuned by a shunt inductor (the configuration shown in Fig. 7 without the impedance transformer). Junction's parasitic capacitance is tuned out at 485 GHz in this configuration. In Fig. 9, the red contour encloses the region on the Smith chart that yields single-side-band (SSB) receiver noise temperature T_{rx} less than 70 K at 485 GHz, where $T_{rx} = T_m + T_{IF}/CG$, T_m is the mixer noise temperature, and CG is the mixer conversion gain. During simulation, the IF amplifier is assumed to have a noise temperature T_{IF} of 15 K, referred to the output of the mixer. It can be seen that low T_{rx} can be achieved over a rather broad area on the Smith chart. The green contour for T_m less than 40 K does not coincide with the contour of T_{rx} because the effects of T_{IF} and CG. On the other hand, the contour of T_m is quite aligned with the transmission efficiency, reflo, from the source to the junction at LO frequencies. reflo is defined here as the portion of available power transmitted to the junction, namely,

$$\text{reflo} = 4\,\mathrm{Re}(Z_s)\,\mathrm{Re}(Z_{inLO\,0})/|Z_s + Z_{inLO\,0}|^2.$$

Fig. 9 also indicates that when the parasitic capacitance is tuned out, the optimum source conductance to give better T_m is around 2.5 (normalized to 1/50 Ω^{-1}), corresponding to Z_s about 20 Ω. This number is again consistent with that given by the empirical formula[5].

Similarly, for the series-inductor-tuned SIS junction configuration shown in Fig. 5, Fig. 10 shows the contours of feed point impedances that gives T_{rx} less than 70 K at several frequencies from 400 to 520 GHz, plotted together with Z_{inLO3}*, the complex conjugate of the input impedance toward the SIS junction after 3 sections of impedance transformers. It is seen that the optimum impedance contours follow the trend of Z_{inLO3}*, with some displacement due to the effect of T_{IF} and CG. Being the complex conjugate, Z_{inLO3}* rotates counter-clockwise on the Smith chart as the frequency is increased, opposite to either Z_{inLO3} or Z_s, which rotates clockwise as frequency is increased. It then becomes impossible to align Z_s with Z_{inLO3}* completely. To achieve good T_{rx} over the entire band, Z_s can be set to be equally distant from the optimum T_{rx} contours. The resulting T_{rx} is shown in Fig. 11 along with the transmission efficiency and the 4 times quantum noise limit as a reference. Similar results, as shown in Fig. 12, can be achieved for the shunt-inductor-tuned configuration. The proximity of the optimum source impedance with Z_{inLO3}*, instead of Z_{in}* at signal frequencies, is attributed to the cancellation of the correlated components of the shot noise[5].

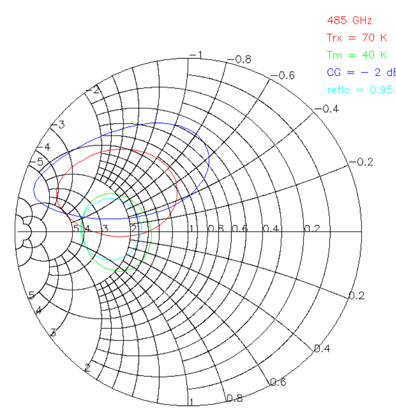

Figure 9. Contours of T_{rx} (red), T_m (green), CG (blue), and reflo (cyan) on an admittance Smith chart for the shunt-inductor-tuned configuration at 485 GHz, where junction's parasitic capacitance is tuned out.

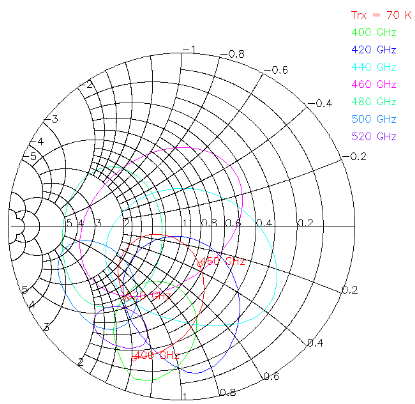

Figure 10. Contours of T_{rx} of the series-inductor-tuned setup at several frequencies, along with the complex conjugate of input impedance of the junction after 3 sections of transmission lines, Z_{inLO3}*.

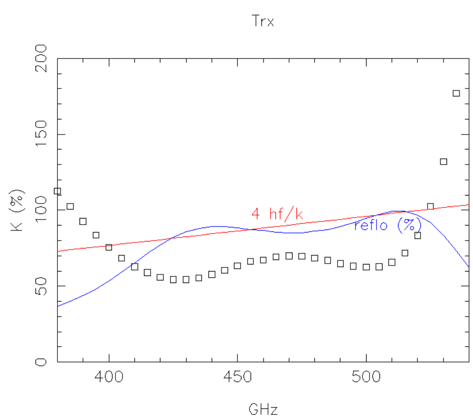

Figure 11. The resulting T_{rx} (square markers) of the mixer design shown in Fig. 5 (series-inductor-tuned). 4 times quantum noise is plotted (red line) as a reference. The transmission efficiency (blue trace) is also shown. It is seen that good reflo corresponds to good T_{rx}, with a little displacement caused by the effect the T_{IF}.

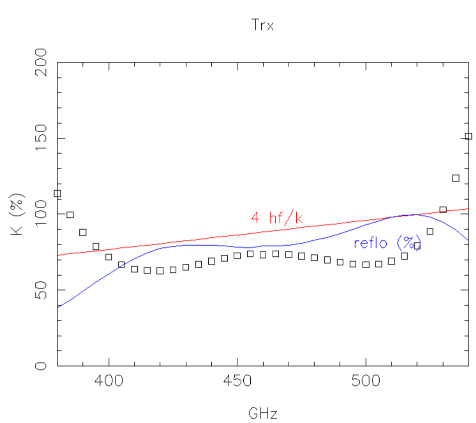

Figure 12. Similar results obtained for the mixer design shown in Fig. 7 (shunt-inductor-tuned).

V. Summary

SIS junction mixers using two tuning schemes were designed for SMA 400 – 520 GHz band. The shunt-inductor-tuned design has the advantage of higher input resistance. The matching between the junction and the probe can be less complicated. However, from simulation, two configurations have similar performances, regarding to either receiver noise temperature or bandwidth. The optimum source impedance for low receiver noise temperature is found to be conjugate matched to the input impedance at LO frequencies Z_{inLO}.

Acknowledgment

The author would like to thank C. E. Tong for the mixer block design.

References

[1] R. Blundell, C. E. Tong, D. C. Papa, R. L. Leombruno, X. Zhang, S. Paine, J. A. Stern, H. G. LeDuc, and B. Bumble, "*A wideband fixed-tuned SIS receiver for 200-GHz Operation,*" IEEE Trans. Microwave Theory and Techniques, vol. 43, pp. 933-937, April 1995.

[2] C. E. Tong, R. Blundell, S. Paine, D. C. Papa, J. Kawamura, X. Zhang, J. A. Stern, and H. G. LeDuc, "*Design and characterization of a 250-350 GHz fixed-tuned superconductor-Insulator-superconductor receiver,*" *IEEE Trans. Microwave Theory and Techniques,* vol. 44, pp. 1548-1556, Sept. 1996.

[3] A. V. Raisanen, W. R. McGrath, D. G. Crete, and P. L. Richards, "*Scaled model measurements of embedding impedances for SIS waveguide mixers,*" *Int. J. Infrared and Millimeter Waves*, vol. 6, pp. 1169-1189, 1985.

[4] A. R. Kerr, "*Some fundamental and practical limits on broadband matching to capacitive devices, and the implications for SIS mixer design,*" *IEEE Trans. Microwave Theory and Techniques,* vol. 43, pp.2-13, Jan. 1995.

[5] Q. Ke, M. J. Feldman, "*Optimum source conductance for high frequency superconducting quasiparticle receivers,*" *IEEE Trans. Microwave Theory and Techniques,* vol. 41, pp.600-604, April 1993.

[6] J. R. Tucker, "*Quantum limited detection in tunnel junction mixers,*" *IEEE Journal of Quantum Electronics*, vol. QE-15, pp.1234-1258, Nov. 1979.

[7] W. H. Chang, "*The inductance of a superconducting strip transmission line,*" *J. Appl. Phys.*, vol. 50, pp.8129-8134, 1979.